

Femtosecond Filaments for Standoff Detection of Explosives

Abdul Kalam Shaik and Venugopal Rao Soma*

Advanced Center of Research in High Energy Materials, University of Hyderabad, Hyderabad - 500 046, India

**E-mail: soma_venu@yahoo.com*

ABSTRACT

In this report, we present our results from various studies to qualitatively discriminate the common military explosives viz. RDX, TNT and HMX in their pure form at a distance of ~6.5 m in standoff mode using femtosecond (fs) filament induced breakdown spectroscopy technique (fs FIBS) together with principal component analysis. A ~30 cm length fs filament obtained by a two-lens configuration was used to interrogate those energetic molecules in the form of pressed pellets (150 mg each). The plasma emissions were collected by a Schmidt-Cassegrain telescope (SCT) from a distance of ~8 m away from the investigation zone. Additionally, a few significant results obtained from the LIBS-based investigations of nitroimidazoles with respect to the standoff distance (~2 m) are discussed. Furthermore, we have also summarised a few important results from our recent investigations of bulk energetic materials in various configurations (including those with fs filaments). The results obtained from various fs FIBS configurations corroborate that the filament generation and its properties, the size and f-number of collection optics influence signal strength in the FIBS technique. These results project the fs FIBS technique as a potential technique for investigations aimed at hazardous materials and harsh environments in the standoff mode.

Keywords: Filament induced breakdown spectroscopy; Explosives; PCA; NE-LIBS; Standoff

1. INTRODUCTION

Discrimination and labelling of high energy materials (HEMs)/explosives is an immediate concern to restrict their illegitimate transport, thwart the terrorist activities and safeguard the civilians¹. Though there are several lab based techniques and electronic sensors for detecting explosives, they are capable of providing only near-field detection (such as optical and chemical based sensors) or limited to the presence of a particular moiety or bond (such as chemiluminescence technique, which cannot identify the non-nitro explosives)². Furthermore, few of these techniques can not provide real-time detection and require sample collection (such as mass spectrometry)³. Consequently, more often than not, safety of the operator as well as the device is at stake. Over the past couple of decades, as an alternative to conventional techniques, several laser-based spectroscopic techniques including Raman spectroscopy, photoacoustic spectroscopy (PAS) and laser induced breakdown spectroscopy (LIBS) are being developed for the identification/discrimination of explosives though with certain limitations^{4,7}. In addition to these techniques, a new standoff spectroscopy detection technique based on quartz tuning fork (QTF) has recently been reported for remote sensing chemical hazards substances⁸, which has significant advantages on traditional microphone based PAS or power meter based reflection spectroscopy⁹⁻¹¹. LIBS is an optical emission spectroscopic technique offering in-situ, multi elemental analysis of various samples in single shot in both

the near-field as well as standoff modes¹²⁻¹⁵. The availability of commercialised and miniaturised nanosecond (ns) lasers has led to compact man-portable¹⁶, handheld LIBS systems and as well as field-deployable standoff systems¹⁷ for the investigation of various samples of interest. Nanosecond laser systems have been widely used to carry out LIBS experiments to investigate organic materials and correlate their molecular structure, especially for explosives, in order to identify them¹⁸⁻²⁰. Since LIBS spectra (unlike the Raman spectra) are not the fingerprints of an organic explosives (containing C, H, N, O) several chemometric techniques have been used in tandem to classify the explosives²¹. Simultaneously explosive fingerprints and traces have been investigated on various surfaces (metallic, organic and inorganic surfaces) using ns lasers up to ~60 m^{22,23}.

Though femtosecond (fs) pulses offer numerous advantages for LIBS studies such as precise interrogation, less heat effected zones^{24,25}, their use has been limited to proximal setups, especially in case of explosive detection²⁶. These (fs) pulses received serious attention after the demonstration of propagation for several hundreds of meters in the form of filaments^{27,28}. The fs pulses were successfully utilised in atmospheric sensing²⁹, and biological simulants³⁰. Laserna³¹, *et al.* from their detailed experimental studies revealed that atmospheric turbulence can affect the divergence and focusing of ns beam leading to beam wandering and a significant reduction in irradiance delivered at remote locations. Long range propagation of high peak-power fs laser pulses has been demonstrated successfully by several groups²⁷. However Jin^{32,33},

et al. have reported the irregular intensity distribution in fs filaments after travelling 20 m in air (500 GW power, $\tau = 60$ fs, beam diameter 30 mm). It was also concluded that filamentation could be controlled by adjusting the beam divergence and laser power. Likewise, detailed studies from Fisher³⁴, *et al.* revealed that the onset of filamentation i.e. position of formation of filament can be controlled by the use of a vortex phase plate element. Chin³⁵, *et al.* demonstrated the elongation of plasma channel generated by temporally shaped fs pulses. The phenomenon of ablation with short pulses (<10 ps) differs from long pulses (ns) and results in different molecular to atomic species intensities. Emissions from molecular species is predominant in fs LIBS than in ns LIBS owing to more fragmentation in former case due to the lack of plasma-pulse reheating and low plasma temperature³⁶. Therefore, employing fs pulses for explosive detection in standoff mode is not only interesting but challenging as well. Here, we demonstrate the discrimination of three explosive molecules of (a) RDX (1,3,5-Trinitro-1,3,5-triazinane) (b) HMX (1,3,5,7-Tetranitro-1,3,5,7-tetrazocane) and (c) TNT (2-methyl-1,3,5-trinitrobenzene) using fs ST-FIBS technique in tandem with principal component analysis (PCA) and importantly at a standoff distance of ~ 6.5 m. Further, various factors influencing the signal strength in the standoff mode as well as the advantage of using nanoparticles for trace investigation of HEMs are discussed systematically from results obtained in various configurations using fs pulses/fs filaments in the form of a mini review.

2. EXPERIMENTAL DETAILS

The schematic presented in Fig. 1 describes the three experimental configurations utilised to investigate the energetic materials. Femtosecond pulses (~ 50 fs at 800 nm, 1 kHz) delivered by an ultrafast Ti:Sapphire laser system (~ 4 mJ total energy, 1 kHz repetition rate) were used to investigate the high energy materials in ambient air. The emissions from laser/filament-induced plasma were coupled through an optical fiber (600 μm core diameter) to a Mechelle 5000 spectrograph attached with an ICCD (possessing a 0.05 nm resolution @ 500 nm). Table 1 summarizes the different types of focusing

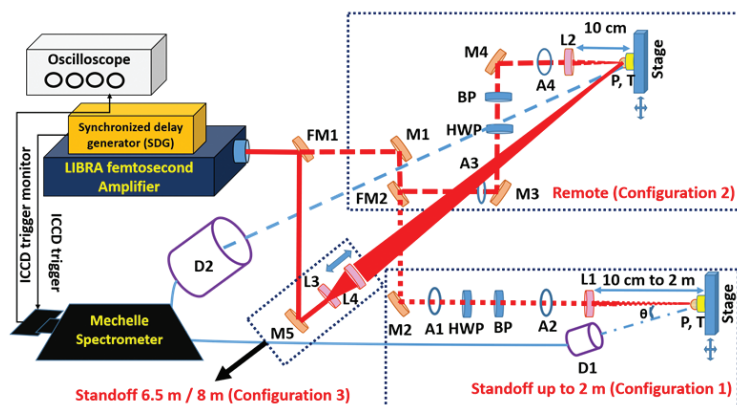


Figure 1. A schematic of the three experimental configurations employed for the investigation of high energy materials (HEMs) using fs pulses (1) fs ST-LIBS1 (up to ~ 2 m), (2) R-LIBS (~ 10 cm/ ~ 8.5 m) and (3) fs ST-FIBS (~ 6.5 m/ ~ 8 m). FM-flip mirror; M-mirror; L-lens; A-aperture; P-plasma; T-target; HWP-half wave plate; BP- Brewster polarizer.

optics, collection optics, the focusing and collection distances employed in all the three configurations. Figures 2(a) and 2(b) respectively show the front view and side view of the collection optics ME-OPT-0007 (D1) and Schmidt-Cassegrain telescope (D2) used in the various configurations. Pellets of pure HEMs powders weighing 150 mg were pressed into pellets of 12 mm diameter, 3 mm thickness using a hydraulic press (Carver Co.) for 10 min at 3-ton pressure.

3. RESULTS AND DISCUSSIONS

Although LIBS is a multi-elemental analysis technique, the spectral data often contains lines resulting from excited atoms and the molecular bands from excited radicals. The molecular bands in the LIBS spectra could result from various scenarios such as (i) formation of excited dimers from the fragmentation of sample during the ablation and (ii) various recombination reactions within the plasma constituents as well as from those between the plasma and ambient constituents. There are several applications of these molecular bands in analysing organic samples (for instance, plastics containing hydrocarbon chains and energetic materials). The LIBS spectra

Table 1. Summary of the various focusing conditions in three different fs LIBS geometries utilised in the present study

Configuration	fs ST-FIBS1	Remote LIBS	fs ST-FIBS2
Beam path in the setup	Dotted line: FM1 (down)-M1-FM2 (down)-M2-A1-HWP-BP-A2-L1-target	Dashed line: FM1 (down)-M1-FM2 (up)-M3-HWP-BP-M4-A3-L2- Target	Solid line: FM1 (up)-M5-L3-L4-Target
Focusing optics	Five lenses of different focal lengths (a) 10 cm (b) 30 cm (c) 50 cm (d) 100 cm (e) 200 cm.	A single plano convex of 10 cm focal length	L3:[PCX (f=100cm, 2"); and L4: PCV (f=-50cm, 2")]
Collecting optics	Andor ME-OPT-0007 (D1); entrance aperture of 2" diameter and f-number equal to f/7; transmission wavelength UV-VIS-NIR region (200-1000 nm)	Schmidt-Cassegrain Telescope (SCT) (D2); entrance aperture of 6" diameter and f-number equal to f/10; transmission wavelength 370-880 nm	Schmidt-Cassegrain Telescope (SCT) (D2)
Focusing length	10 cm, 30 cm, 50 cm, 100 cm, 200 cm.	10 cm	~ 6.5 m (the distance between L4 and target)
Collection length	(a) 10 cm (b) 30 cm (c) 50 cm (d) 100 cm (e) 200 cm in such a way that both focusing and collection distances are the same.	~ 8.5 m (target to the SCT)	~ 8 m (distance between target and SCT)

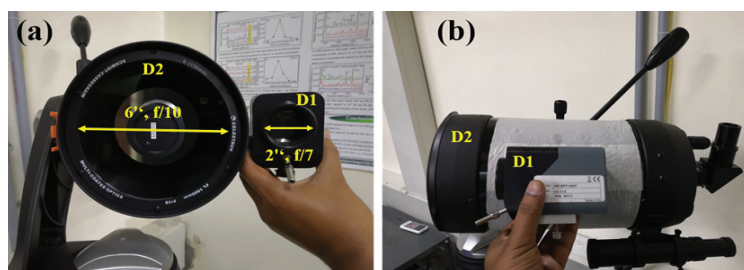


Figure 2. Front view (a) and side view (b) of collection optics ME-OPT-0007 (D1) and Schmidt-Cassegrain telescopes (D2) for the comparison of entrance aperture and sizes.

of organic explosives are analogous to that of plastics due to similar atomic constituents i.e. C, H, N and O. The LIBS spectra of pure organic high energy materials were composed of molecular emission bands of (a) CN violet bands ($B^2\Sigma^+ \rightarrow X^2\Sigma^+$) [in the spectral region 358-420 nm corresponding to Δv values of 1, 0, -1 respectively] (b) C_2 swan bands ($d^3\Pi_g \rightarrow a^3\Pi_u$) [in the spectral range of 465-565 nm with maximum intensity at $\Delta v=0$] along with the atomic emissions of C, H, N and O. The atomic peaks and molecular bands were identified using the NIST database³⁷ and Gaydon and Pearse molecular database (handbook)³⁸, respectively.

3.1 Results from fs ST-FIBS1 (configuration 1) and Remote-LIBS (configuration 2)

A set of five (5) imidazole molecules (energetic molecules developed in-house) were investigated in at five different standoff positions using fs ST-FIBS1 setup³⁹. Thus five plano-convex lenses of different focal lengths (i.e. 10 cm, 30 cm, 50 cm, 100 cm, and 200 cm) were utilised to focus the fs laser pulses on to the sample and to create the plasma while the emissions were collected by D1. The detector D1 was fixed adjacent to the focusing lens and was moved, adjusted/tilted for each of the standoff distances so that the collection distance was identical to focusing distance. When the fs pulses were focused by long focal length lenses [$f > 30$ cm] a filament of ~2 cm to ~10 cm was witnessed. At each position 15-20 FIBS spectra of each sample (in pure pellet form) were recorded. FIBS spectra of a series of nitroimidazoles recorded at each position in the fs ST-FIBS1 configuration were reported in our earlier work³⁹. The spectra of energetic molecules were

composed of C, N, H, and O atomic emissions and CN, C_2 molecular emissions. Further, we could discriminate all the five molecules using principle component analysis (PCA) of the FIBS data.

We observed that the spectral intensity of all plasma constituents decreased as the collection distance increased. Figures 3(a), 3(b) illustrate the decrease in the intensity of C I (247.8 nm) atomic emission and CN molecular band head at 388.4 nm of 4nitro-imidazole with respect to increase in the standoff distance. Both the intensities were fitted to exponential decay (e^{-x}) and inverse square decay ($1/x^2$) where 'x' is the standoff distance. From Figs. 3(a) and 3(b) data it is obvious that the emissions decayed exponentially with R^2 value being higher for the exponential decay. Figure 3(c) depicts the trend of signal-to-noise ratio (SNR) associated with carbon atomic emission and CN molecular band head for the 4-NIm molecule. The SNR of C atomic emission decayed exponentially whereas the SNR associated with CN emissions did not change much. This could be attributed to the fs filament interaction, which results in low plasma temperatures favoring molecular formation rather the atomisation of radicles. Further, the decrease in the SNR could be related to (a) a decrease in the detector solid angle (b) a decrease in the intensity delivered at the focal region due to increase in the spot-size and (c) a decrease in the energy per unit length of the filament.

In the remote-LIBS setup (configuration 2) the proof of concept of collection of plasma emissions from a far distance (~8.5 m) was demonstrated by investigating metals and HEMs (nitro-imidazoles and nitro-pyrazoles) and were successfully discriminated using PCA³⁹. The first three PCs contributing for the classification was 88 %, which is essentially equal to the contribution of PCs at 30 cm in ST-FIBS1 configuration with D1 as collection optics. The increase in the efficiency of PCs can be attributed to the increase in aperture size of the telescope which subtends larger solid angle at the plasma source. The results corroborate the usage of telescopes with large entrance aperture for overcoming the difficulties associated with small collection optics while working on standoff investigations.

3.2 Discrimination of HEMs in ST-FIBS2 (Configuration 3) using Femtosecond Filaments

After demonstrating the discrimination of energetic/explosive materials in remote mode, the limitation of focusing

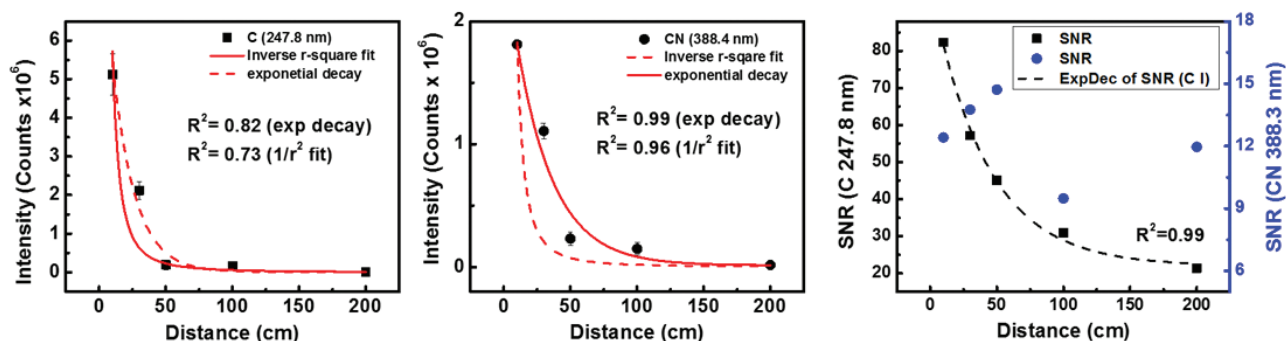


Figure 3. Decrease in the intensity of (a) C I atomic emission (C I 247.8 nm), (b) CN molecular band head at 388.4 nm, and (c) Trend in the signal-to-noise ratio (SNR) of C I atomic emission [black squares] and CN molecular band head [blue circles] of 4nitro-imidazole.

fs pulses at a fixed position using a single lens was circumvented by using a combination of two lenses i.e. a plano-concave lens (denoted as PCV, $f = -50$ cm, 2" diameter) to diverge the fs pulses and a plano-convex lens (denoted as PCX, $f = 100$ cm, 2" diameter) to converge them back. The advantage of such combined lens system is that the onset of filamentation can be controlled and the filaments can be focused at any desired location. Depending on the lens combinations one can focus the pulses at few meters to few hundreds of meters. We had earlier successfully investigated bimetallic targets (Ag@Au, Ag@Cu)⁴⁰ and a set of six energetic imidazoles⁴¹ in the same configuration. In both cases we could achieve excellent discrimination using the PCA.

3.2.1 Discrimination of RDX, HMX and TNT using PCA

RDX, TNT, and HMX are the three explosive molecules that have been explicitly used in military ammunitions and landmines. It is very essential to detect these molecules in real time. The fs ST-FIBS2 spectra of these molecules were acquired with a gate delay of 50 ns, a gate width of 1 μ s and an exposure time of 1.5 s combined with an ICCD gain of 3000 and a total of 6 accumulations. Typical ST-FIBS2 spectrum of these molecules (out of 10-15 spectra) are reported in our earlier work⁴². The ST-FIBS2 spectra consisted of only CN ($\Delta v=0$) band with band head at 388.34 nm. The absence of carbon atomic emission line (C I) at 247.8 nm could be ascribed to the limitation of SCT (D2) where only visible/NIR radiation is transmitted. The absence of other atomic lines such as H, N and O could be related the minimal breakdown of the air surrounding the fs plasma. Further, the low plasma temperatures generated in filament interaction could limit the time of persistence of these atomic transitions.

The fs ST-FIBS spectra were analysed with principal component analysis (PCA) code developed in-house (and written in MATLAB). PCA reduces the multivariate data to the few dimensions. Only the CN ($\Delta v=0$) band head in the 385-389 nm spectral region was considered for the analysis as the other atomic signatures such as C, H and O were absent. Figure 4(a) illustrates the 3D score plot and 4(b) presents the principal components (PCs) obtained from the PCA analysis. The first three PCs obtained in the PCA analysis accounted for 88% (85%, 2%, and 1%) of the total variance existing in the data set

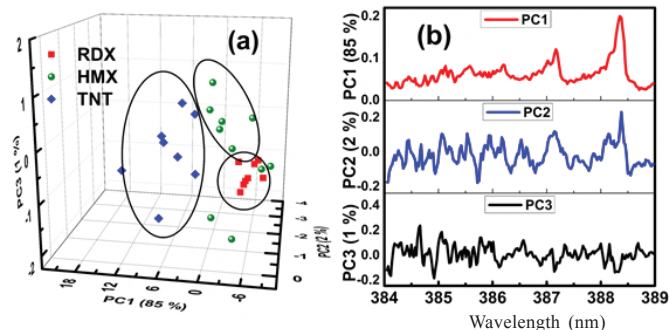


Figure 4. (a) 3-D score plot and (b) first three PCs representing the important spectral features for the discrimination obtained from the principal component analysis (PCA) of ST-FIBS2 spectra of RDX, TNT and HMX.

3.2.2 Investigation of Enhancement in the LIBS/FIBS Signal of Bulk and Trace Explosives

Several improvisations in LIBS methodology have been projected to improve the sensitivity of LIBS which include but not limited to double pulse LIBS, resonance LIBS, and various hyphenated or hybrid techniques where magnetic field or spark were generated to improve the signal strength and, consequently, led to an increase in the Limit of detections⁴³⁻⁴⁵. However, employing these techniques makes the system bulkier with increased level of difficulty to operate. Recently nanoparticle enhanced LIBS (NE-LIBS) technique has received attention from several research groups owing to its as it is execution and setup, availability of various plasmonic and metallic NPs where the enhancement in analyte signal was achieved using nanoparticles⁴⁶⁻⁵⁰. After achieving an enhancement by a factor of two in the Cu LIBS signal using Ag NPs (obtained with fs pulses) in near-field⁵¹, we could achieve (and recently reported) a two-factor enhancement in (a) LIBS signal of HEMs i.e. nitroamino (NHNO₂) substituted aryl-tetrazole in near-field configuration and (b) FIBS signal of TNT recorded in the standoff mode through drop-casting 10 μ l of Ag nanospheres [stabilised in citrate solution as shown in Fig. 5(a)]. Furthermore, the potential of fs filaments was demonstrated for investigating explosive traces in ST-FIBS2 setup at ~ 6.5 m by investigating a residue of CL-20 on a brass substrate as a proof of concept⁴¹.

To achieve a 50 mM solution, 22 mg of CL-20 powder was dissolved in 1 ml of acetone. A 50 μ l (1 mg) was drop-casted on a brass target which was spread over an area of 1 cm². After five minutes we observed that a layer of CL-20 residue was formed at room temperature [due to evaporation of acetone]. An enhancement in the CN (388.34 nm) peak in the presence of standard Ag NPs [Fig. 5(b)] was observed confirming the presence of CL-20. However, in the absence of NPs we did not observe any CN band (typical signature of an organic energetic molecule). This clearly demonstrates that using NPs is an efficient alternative to detect traces⁴⁴. The enhancements in the LIBS signal in the presence of NPs has been accredited to the electromagnetic field enhancement. This

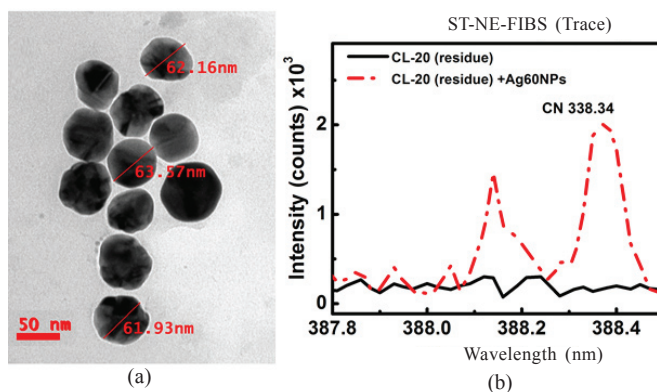


Figure 5. (a) TEM micrograph of 60 nm Ag nanospheres (NanoXact, 0.02 mg/ml) (b) Uncovering of CN spectral signature at 388.34 nm of a CL-20 residue (1 mg/1 cm²) using AgNPs in standoff mode (~ 6.5 m)⁴¹.

(© Re-printed with permission from OSA, *OSA Continuum*, 2019, 2(3), 554-562)

field enhancement can essentially upsurge the LIBS emission signal up to 100 times with respect to the LIBS signal of a sample ablated using normal conditions⁴⁶. It is believed that the NPs over the surface act as impurities thereby decreasing the optical breakdown threshold. Furthermore, they act as ignition centers and providing more seed electrons which improves the ablation efficiency resulting in the increased LIBS signal⁵². Thus NE-LIBS could be considered as a promising variant of LIBS for several applications especially in trace detection of explosives in both proximal and standoff configurations. Further, the potential of FIBS technique has the potential to extend to other important fields as well. For example, Burger⁵³, *et al.* have achieved the remote detection (10 m) of uranium using femtosecond filaments. They studied the effect of the femtosecond pulse chirp on the signals obtained. They recommend the usage of adaptive optics for further optimisation of the FIBS.

4. CONCLUSIONS AND FUTURE SCOPE

In the present article, the analytical capability of femtosecond filaments towards investigating energetic molecules/explosives is presented in the form of a mini-review. The systematic development of fs ST-FIBS setup highlighting the importance of filament generation conditions and properties of collection optics are also summarised. The application of fs FIBS in combination with PCA for the investigation/discrimination of explosive molecules RDX, HMX and TNT in the form of pellets (~150 mg) at a standoff distance of ~6.5 m is demonstrated. Though trace (1 mg/1 cm²) explosive (CL-20) has been detected from ~6.5 m further studies are warranted to evaluate the potential of NE-FIBS for the trace detection of HEMs with primary focus on (a) optimising the laser energy, (b) spectral acquisition parameters and (c) type and propagation properties of filaments. This is because these parameters affect the LIBS plasma for standoff and trace analysis of any hazardous materials. Additionally, developing superior semi-supervised/supervised and/or machine learning based algorithms will help in not only distinguishing the explosives but also for unambiguous identification and labelling⁵⁴⁻⁵⁵.

REFERENCES

- Pellegrino, P. M.; Holthoff, E. L. & Farrell, M. E. Laser-based optical detection of explosives. CRC Press, 2015, 383 p.
- Singh, S. Sensors - An effective approach for the detection of explosives. *J. Hazard. Mater.*, 2007, **144**(1), 15-28. doi:10.1016/j.jhazmat.2007.02.018.
- Caygill, J. S.; Davis, F. & Higson, S. P. Current trends in explosive detection techniques. *Talanta*, 2012, **88**, 14-29. doi:10.1016/j.talanta.2011.11.043.
- Fountain, A.W.; Christesen, S.D.; Moon, R.P.; Guicheteau, J.A. & Emmons, E.D. Recent advances and remaining challenges for the spectroscopic detection of explosive threats. *Appl. Spectrosc.*, 2014, **68**(8), 795-811. doi:10.1366/14-07560.
- Wallin, S.; Pettersson, A.; Östmark, H. & Hobro, A. Laser-based standoff detection of explosives: A critical review. *Anal. Bioanal. Chem.*, 2009, **395**(2), 259-274. doi:10.1007/s00216-009-2844-3.
- Wen, P.; Amin, M.; Herzog, W.D. & Kunz, R.R. Key challenges and prospects for optical standoff trace detection of explosives. *Trends Anal. Chem.*, 2018, **100**, 136-144. doi:10.1016/j.trac.2017.12.014.
- Kalam, S.A.; Rao, S. & Rao, S.V. Standoff LIBS for explosives detection-challenges and status. *Laser Focus World*, April, 2017), 24-28.
- Li, J.; Liu, N.; Ding, J.; Zhou, S.; He, T. & Zhang, L. Piezoelectric effect-based detector for spectroscopic application. *Optics Lasers Eng.*, 2019, **115**, 141-148. doi: 10.1016/j.optlaseng.2018.11.020.
- Marcus, L.S.; Holthoff, E.L. & Pellegrino, P.M. Standoff photoacoustic spectroscopy of explosives. *Appl. Spectrosc.*, 2017, **71**(5), 833-838. doi:10.1177/0003702816654168.
- Cui, Y.-T.; Ma, E.Y. & Shen, Z.-X. Quartz tuning fork based microwave impedance microscopy. *Rev. Sci. Instrum.*, 2016, **87**(6), 063711. doi:10.1063/1.4954156.
- Zrimsek, A.B.; Bykov, S.V. & Asher, S. A. Deep ultraviolet standoff photoacoustic spectroscopy of trace explosives. *Appl. Spectrosc.*, 2019, **73**(6), 601-609. doi:10.1177/0003702818792289.
- Baudelet, M. & Smith, B.W. The first years of laser-induced breakdown spectroscopy. *J. Anal. At. Spectrom.*, 2013, **28**(5), 624-629. doi:10.1039/C3JA50027F.
- Qing-Yu, L. & Yi-Xiang, D. Laser-induced breakdown spectroscopy: From experimental platform to field instrument. *Chin. J. Anal. Chem.*, 2017, **45**(9), 1405-1414. doi:10.1016/S1872-2040(17)61040-5.
- Rao, S.V.; Kalam, S.A. & Bharathi, M.S.S. Photonics for explosives detection. *Digital Encyclopedia of Applied Physics* (2019), pp. 1-31
- Moros, J. & Laserna, J. Laser-induced breakdown spectroscopy (LIBS) of organic compounds: A review. *Appl. Spectrosc.*, 2019, **73**(9), 963-1011.
- DeLucia, F.; Samuels, A.C.; Harmon, R.S.; Walters, R.A.; McNesby, K.L.; LaPointe, A.; Winkel, R. & Miziolek, A.W. Laser-induced breakdown spectroscopy (LIBS): a promising versatile chemical sensor technology for hazardous material detection. *IEEE Sens. J.*, 2005, **5**(4), 681-689. doi: 10.1109/JSEN.2005.848151.
- Lopez-Moreno, C.; Palanco, S.; Laserna, J.J.; DeLucia Jr, F.; Miziolek, A.W.; Rose, J.; Walters, R.A. & Whitehouse, A.I. Test of a stand-off laser-induced breakdown spectroscopy sensor for the detection of explosive residues on solid surfaces. *J. Anal. At. Spectrom.*, 2006, **21**(1), 55-60. doi:10.1039/B508055J.
- Gundawar, M.K.; Junjuri, R. & Myakalwar, A.K. Standoff detection of explosives at 1 m using laser induced breakdown spectroscopy. *Def. Sci. J.*, 2017, **67**(6), 623-630.

- doi: 10.14429/dsj.67.11498.
19. Sunku, S.; Gundawar, M. K.; Myakalwar, A. K.; Kiran, P. P.; Tewari, S. P. & Rao, S. V. Femtosecond and nanosecond laser induced breakdown spectroscopic studies of NTO, HMX, and RDX, *Spectrochim. Acta, Part B*, 2013, **79**, 31-38.
doi:10.1016/j.sab.2012.11.002.
 20. Rao, E.N.; Mathi, P.; Kalam, S. A.; Sreedhar, S.; Singh, A. K.; Jagatap, B. & Rao, S. V. Femtosecond and nanosecond LIBS studies of nitroimidazoles: correlation between molecular structure and LIBS data. *J. Anal. At. Spectrom.*, 2016, **31**(3), 737-750.
doi:10.1039/C5JA00445D.
 21. Myakalwar, A. K.; Dingari, N. C.; Dasari, R. R.; Barman, I. & Gundawar, M. K. Non-gated laser induced breakdown spectroscopy provides a powerful segmentation tool on concomitant treatment of characteristic and continuum emission. *PLoS one*, 2014, **9**(8), e103546.
doi:10.1371/journal.pone.0103546.
 22. Lucena, P.; Gaona, I.; Moros, J. & Laserna, J. Location and detection of explosive-contaminated human fingerprints on distant targets using standoff laser-induced breakdown spectroscopy. *Spectrochim. Acta, Part B*, 2013, **85**, 71-77.
doi:10.1016/j.sab.2013.04.003.
 23. Gaona, I.; Serrano, J.; Moros, J. & Laserna, J.J. Range-adaptive standoff recognition of explosive fingerprints on solid surfaces using a supervised learning method and laser-induced breakdown spectroscopy. *Anal. Chem.*, 2014, **86**(10), 5045-5052.
doi:10.1021/ac500694j.
 24. Labutin, T.A.; Lednev, V.N.; Ilyin, A.A. & Popov, A.M. Femtosecond laser-induced breakdown spectroscopy. *J. Anal. At. Spectrom.*, 2016, **31**(1), 90-118.
doi:10.1039/C5JA00301F.
 25. Harilal, S.S.; Yeak, J.; Brumfield, B.E.; Suter, J.D. & Phillips, M.C. Dynamics of molecular emission features from nanosecond, femtosecond laser and filament ablation plasmas. *J. Anal. At. Spectrom.*, 2016, **31**(6), 1192-1197.
doi:10.1039/C6JA00036C.
 26. De Lucia, F.C.; Gottfried, J.L. & Miziolek, A.W. Evaluation of femtosecond laser-induced breakdown spectroscopy for explosive residue detection. *Opt. Express*, 2009, **17**(2), 419-425.
doi:10.1364/OE.17.000419.
 27. Rodriguez, M.; Bourayou, R.; Méjean, G.; Kasparian, J.; Yu, J.; Salmon, E.; Scholz, A.; Stecklum, B.; Eislöffel, J. & Laux, U. Kilometer-range nonlinear propagation of femtosecond laser pulses. *Phys. Rev. E*, 2004, **69**(3), 036607.
doi:10.1103/PhysRevE.69.036607.
 28. Stelmaszczyk, K.; Rohwetter, P.; Méjean, G.; Yu, J.; Salmon, E.; Kasparian, J.; Ackermann, R.; Wolf, J.-P. & Wöste, L. Long-distance remote laser-induced breakdown spectroscopy using filamentation in air. *Appl. Phys. Lett.*, 2004, **85**(18), 3977-3979.
doi:10.1063/1.1812843.
 29. Xu, H.L. & Chin, S.L. Femtosecond laser filamentation for atmospheric sensing. *Sens.*, 2011, **11**(1), 32-53.
doi:10.3390%2Fs110100032.
 30. Baudelet, M., Richardson, M. & Sigman, M., Self-channeling of femtosecond laser pulses for rapid and efficient standoff detection of energetic materials. In 2009 IEEE Conference on Technologies for Homeland Security, (IEEE, 2009), 472-476.
doi: 10.1109/THS.2009.5168075.
 31. Laserna, J.; Reyes, R. F.; González, R.; Tobaría, L. & Lucena, P. Study on the effect of beam propagation through atmospheric turbulence on standoff nanosecond laser induced breakdown spectroscopy measurements. *Opt. Express*, 2009, **17**(12), 10265-10276.
doi:10.1364/OE.17.010265.
 32. Jin, Z.; Zhang, J.; Xu, M.; Lu, X.; Li, Y.; Wang, Z.; Wei, Z.; Yuan, X. & Yu, W. Control of filamentation induced by femtosecond laser pulses propagating in air. *Opt. Express*, 2005, **13**(25), 10424-10430.
doi:10.1364/OPEX.13.010424.
 33. Chin, S.; Hosseini, S.; Liu, W.; Luo, Q.; Théberge, F.; Aközbek, N.; Becker, A.; Kandidov, V.; Kosareva, O. & Schröder, H. The propagation of powerful femtosecond laser pulses in optical media: physics, applications, and new challenges. *Can. J. Phys.*, 2005, **83**(9), 863-905.
doi:10.1139/p05-048.
 34. Fisher, M.; Siders, C.; Johnson, E.; Rusyak, O.; Brown, C. & Richardson, M. Control of filamentation for enhancing remote detection with laser induced breakdown spectroscopy. In Enabling Technologies and Design of Nonlethal Weapons, (International Society for Optics and Photonics, 2006), 621907.
doi:10.1117/12.663824.
 35. Chen, A.; Li, S.; Qi, H.; Jiang, Y.; Hu, Z.; Huang, X. & Jin, M. Elongation of plasma channel generated by temporally shaped femtosecond laser pulse. *Opt. Commun.*, 2017, **383**, 144-147.
doi:10.1016/j.optcom.2016.08.079.
 36. Kalam, S.A.; Murthy, N.L.; Mathi, P.; Kommu, N.; Singh, A.K. & Rao, S.V. Correlation of molecular, atomic emissions with detonation parameters in femtosecond and nanosecond LIBS plasma of high energy materials. *J. Anal. At. Spectrom.*, 2017, **32**(8), 1535-1546.
doi:10.1039/C7JA00136C.
 37. NIST, Atomic spectra database. <https://www.nist.gov/pml/atomic-spectra-database>. (Accessed on 8/14/2019)
 38. Gaydon, A. G. & Pearse, R. The identification of molecular spectra. Springer Netherlands, 1976. 407 p.
 39. Shaik, A.K.; Epuru, N.R.; Syed, H.; Byram, C. & Soma, V.R. Femtosecond laser induced breakdown spectroscopy based standoff detection of explosives and discrimination using principal component analysis. *Opt. Express*, 2018, **26**(7), 8069-8083.
doi:10.1364/OE.26.008069.
 40. Shaik, A.K. & Soma, V.R. Discrimination of bimetallic alloy targets using femtosecond filament-induced breakdown spectroscopy in standoff mode. *Opt. Lett.*, 2018, **43**(15), 3465-3468.
doi:10.1364/OL.43.003465.

41. Shaik, A.K. & Soma, V.R. Standoff discrimination and trace detection of explosive molecules using femtosecond filament induced breakdown spectroscopy combined with silver nanoparticles. *OSA Continuum.*, 2019, **2**(3), 554-562.
doi:10.1364/OSAC.2.000554.
42. Shaik, A. K. & Soma, V. R. Standoff detection of RDX, TNT, and HMX using femtosecond filament induced breakdown spectroscopy. *In Light, Energy and the Environment 2018 (E2, FTS, HISE, SOLAR, SSL)*, OSA Technical Digest (Optical Society of America, 2018), paper JW4A.1.
doi:10.1364/FTS.2018.JW4A.1.
43. Moore, D.S. Instrumentation for trace detection of high explosives. *Rev. Sci. Instrum.*, 2004, **75**(8), 2499-2512.
doi:10.1063/1.1771493.
44. Hahn, D. W. & Omenetto, N. Laser-induced breakdown spectroscopy (LIBS), part I: Review of basic diagnostics and plasma-particle interactions: still-challenging issues within the analytical plasma community. *Appl. Spectrosc.*, 2010, **64**(12), 335A-366A.
doi: 10.1366/000370210793561691.
45. Hahn, D. W. & Omenetto, N. Laser-induced breakdown spectroscopy (LIBS), part II: review of instrumental and methodological approaches to material analysis and applications to different fields. *Appl. Spectrosc.*, 2012, **66**(4), 347-419.
doi: 10.1366/11-06574.
46. De Giacomo, A.; Gaudiuso, R.; Koral, C.; Dell'Aglio, M. & De Pascale, O. Nanoparticle-enhanced laser-induced breakdown spectroscopy of metallic samples. *Anal. Chem.*, 2013, **85**(21), 10180-10187.
doi:10.1021/ac4016165.
47. Sherbini, A. M. E. & Parigger, C. G. Nano-material size dependent laser-plasma thresholds. *Spectrochim. Acta, Part B*, 2016, **124**, 79-81.
doi:10.1016/j.sab.2016.08.015.
48. Koral, C.; Dell'Aglio, M.; Gaudiuso, R.; Alrifai, R.; Torelli, M. & De Giacomo, A. Nanoparticle-enhanced laser induced breakdown spectroscopy for the noninvasive analysis of transparent samples and gemstones. *Talanta*, 2018, **182**, 253-258.
doi:10.1016/j.talanta.2018.02.001.
49. Sanchez-Ake, C.; Garcia-Fernandez, T.; Benitez, J. L.; de la Mora, M. B. & Villagran-Muniz, M. Intensity enhancement of LIBS of glass by using Au thin films and nanoparticles. *Spectrochim Acta B*, 2018, **146**, 77-83.
doi:10.1016/j.sab.2018.05.007.
50. De Giacomo, A.; Koral, C.; Valenza, G.; Gaudiuso, R. & Dell'Aglio, M. Nanoparticle enhanced laser-induced breakdown spectroscopy for microdrop analysis at subppm level. *Anal. Chem.*, 2016, **88**(10), 5251-5257.
doi:10.1021/acs.analchem.6b00324.
51. Kalam, S. A.; Murthy, N. L.; Krishna, J. R.; Srikanth, V. V. S. S. & Rao, S. V. Nanoparticle enhanced laser induced breakdown spectroscopy with femtosecond pulses. *In 13th International Conference on Fiber Optics and Photonics*. OSA Technical Digest (online) (Optical Society of America, 2016), Th3A.89.
doi:10.1364/PHOTONICS.2016.Th3A.89.
52. De Giacomo, A.; Gaudiuso, R.; Koral, C.; Dell'Aglio, M. & De Pascale, O. Nanoparticle enhanced laser induced breakdown spectroscopy: Effect of nanoparticles deposited on sample surface on laser ablation and plasma emission. *Spectrochim. Acta, Part B*, 2014, **98**, 19-27.
doi: 10.1016/j.sab.2014.05.010.
53. Burger, M.; Skrodzki, P.J.; Finney, L.A.; Nees, J. & Jovanovi, I. Remote detection of uranium using self-focusing intense femtosecond laser pulses. *Remote Sensing*, 2020, **12**, 1281.
54. Wang, Q.; Teng, G.; Li, C.; Zhao, Y. & Peng, Z. Identification and classification of explosives using semi-supervised learning and laser-induced breakdown spectroscopy. *J. Hazard. Mater.*, 2019, **369**, 423-429.
doi:10.1016/j.jhazmat.2019.02.015.
55. Teng, G. E.; Wang, Q. Q.; Kong, J. L.; Dong, L. Q.; Cui, X. T.; Liu, W. W.; Wei, K. & Xiangli, W. T. Extending the spectral database of laser-induced breakdown spectroscopy with generative adversarial nets. *Opt. Express*, 2019, **27**(5), 6958-6969.
doi:10.1364/OE.27.006958.

ACKNOWLEDGEMENT

Authors acknowledge the financial support from DRDO, India [#ERIP/ER/1501138/M/01/319/D (R&D)].

CONTRIBUTORS

Dr Abdul Kalam S. has received his PhD from ACRHEM (School of Physics), University of Hyderabad. He is currently working as a Research Associate at Advanced Center of Research in High Energy Materials, University of Hyderabad, Hyderabad. His major research interests lie in the field of laser matter interaction, plasma spectroscopy, surface enhanced Raman spectroscopy, nonlinear optics, and multivariate analysis. Contribution in the current study, he has performed the experiments in all the configurations, analysed the data, wrote the first draft and improved it over several revisions.

Prof. S. Venugopal Rao obtained his Master's and PhD from University of Hyderabad, India in 1994 and 2000, respectively. He has established state-of-the-art ultrafast laser laboratories at Advanced Center of Research in High Energy Materials, University of Hyderabad, Hyderabad. His research interests include detection of explosives using the techniques of SERS, LIBS, CARS and ultrafast laser-matter interaction. He has published 1 book, 10 book chapters, and more than 275 papers in journals and conference proceedings. Contribution in the current study, he has conceptualised, planned and supervised the experiments and improved the manuscript through valuable suggestions.